

# Glycoform Separation and Characterization of Cetuximab Variants by Middle-up Off-Line Capillary Zone Electrophoresis-UV/Electrospray Ionization-MS

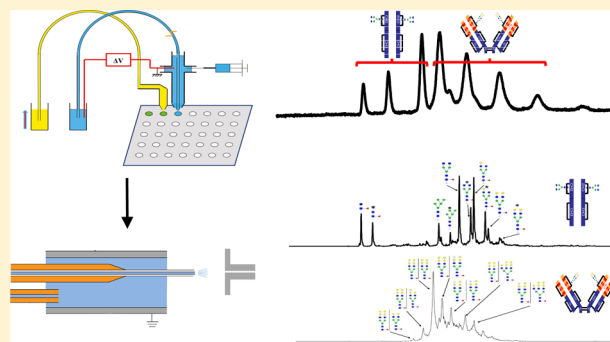
Michael Biacchi,<sup>†</sup> Rabah Gahoual,<sup>†</sup> Nassur Said,<sup>†</sup> Alain Beck,<sup>‡</sup> Emmanuelle Leize-Wagner,<sup>†</sup> and Yannis-Nicolas François<sup>\*,†</sup>

<sup>†</sup>Laboratoire de Spectrométrie de Masse des Interactions et des Systèmes (LSMIS), UDS-CNRS UMR 7140, Université de Strasbourg, Strasbourg 67000, France

<sup>‡</sup>Centre d'Immunologie Pierre Fabre, Saint-Julien-en-Genevois 74164, France

## Supporting Information

**ABSTRACT:** Monoclonal antibodies (mAbs) are highly complex glycoproteins that present a wide range of microheterogeneities that requires multiple analytical methods for full structure assessment and quality control. Capillary zone electrophoresis-mass spectrometry (CZE-MS) couplings, especially by electrospray ionization (ESI), appear to be really attractive methods for the characterization of biological samples. However, due to the presence of non- or medium volatile salts in the background electrolyte (BGE), online CZE-ESI-MS coupling is difficult to implement for mAbs isoforms separation. Here, we report an original strategy to perform off-line CZE-ESI-MS using CZE-UV/fraction collection technology to perform CZE separation, followed by ESI-MS infusion of the different fractions using the capillary electrophoresis-electrospray ionization (CESI) interface as the nanoESI infusion platform. As the aim is to conserve electrophoretic resolution and complete compatibility with ESI-MS without sample treatment, hydroxypropylcellulose (HPC) coated capillary was used to prevent analyte adsorption and asymmetric CZE conditions involving different BGE at both ends of the capillary have been developed. The efficiency of our strategy was validated with the separation of Cetuximab charge variant by the middle-up approach. Molecular weights were measured for six charge variants detected in the CZE separation of Cetuximab subunits. The first three peaks correspond to Fc/2 variants with electrophoretic resolution up to 2.10, and the last three peaks correspond to F(ab')<sub>2</sub> variants with average electrophoretic resolution of 1.05. Two Fc/2 C-terminal lysine variants were identified and separated. Moreover, separation of Fc/2 fragments allowed the glycoprofiling of the variants with the characterization of 7 different glycoforms. Regarding the F(ab')<sub>2</sub> domain, 8 glycoforms were detected and separated in three different peaks following the presence of N-glycolyl neuraminic acid residues in some glycan structures. This work highlights the potential of CZE technology to perform separation of mAbs especially when they carry sialic acid carbohydrates.



Since 1986 and the approbation of muromonab-CD3 by the US Food and Drug Administration (FDA), monoclonal antibodies (mAbs) have taken a major market share in the pharmaceutical industry and their development is constantly increasing.<sup>1,2</sup> mAbs are highly complex glycoproteins potentially displaying many naturally occurring molecular microheterogeneities.<sup>3,4</sup> Patents protecting the first generation blockbuster mAbs will expire in the next 5 years, giving the opportunity to many companies to produce “biogeneric versions”. These copies are referred as biosimilars. Biosimilarity assessment includes extensive physicochemical characterization likewise pharmacokinetic (PK) and pharmacodynamics (PD) study, performed in a comprehensive manner. Analytical high similarity is the most robust scientific basis for comparing independently sourced biologics.<sup>5</sup> As different structural heterogeneities emerged from

comparison of a biosimilar candidate with the reference molecule, more complementary studies should be performed in order to demonstrate the absence of toxicological and negative clinical outcome.<sup>6</sup>

As a consequence, there is a continuous need for improvement of analytical methods to enable fast and accurate characterization. Mass spectrometry (MS), generally coupled with separation methods such as high-performance liquid chromatography (HPLC), plays a key role in the characterization of therapeutic mAbs.<sup>7</sup> Many levels of characterization are performed following different strategies as intact molecular weight (MW) measurement,

Received: March 9, 2015

Accepted: May 13, 2015

Published: May 13, 2015

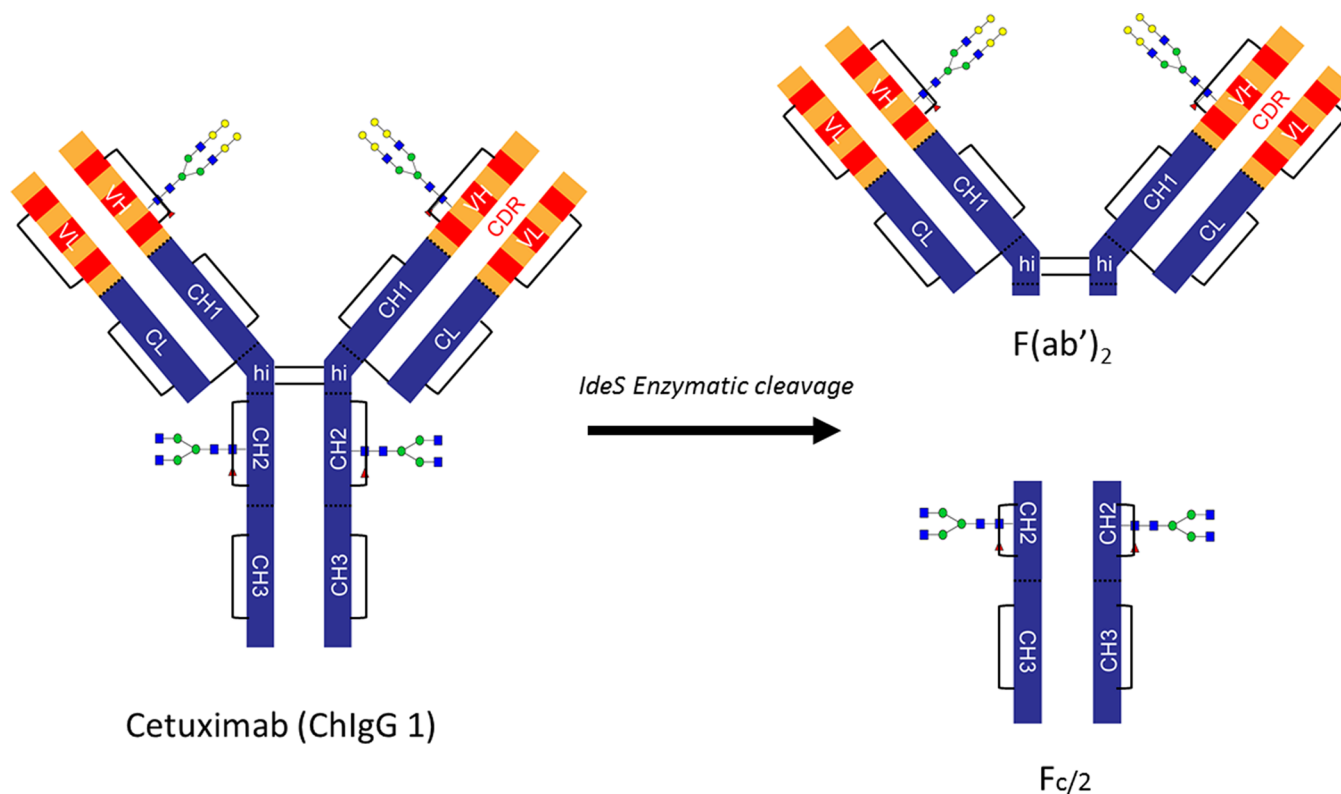


**Figure 1.** Schematic representation IdeS enzymatic cleavage of Cetuximab. Cetuximab is a chimeric IgG: human amino acids are highlighted in blue (constant domains), murine amino acids in orange (frameworks) and in red (the complementary determining region).

top-down, middle-up, and bottom-up approaches.<sup>7–9</sup> Concerning glycosylation variants, which are known as an important class of modification that can significantly impact the immunogenic properties of mAbs,<sup>10</sup> intact MW and middle-up on the domain level as well as bottom-up techniques were also performed.<sup>11–14</sup> However, at this point, no separation of mAbs glycoforms was obtained by HPLC-MS with an intact MW or a middle-up approach.<sup>15–17</sup> As an alternative to HPLC, capillary zone electrophoresis (CZE) has been demonstrated to be a useful and powerful separation method for the characterization of intact proteins.<sup>18,19</sup> CZE and related methods using optical detections were fully established at all stages of mAbs discovery. However, due to the presence of a high concentration of nonvolatile salts in the background electrolyte (BGE) necessary for mAbs variants separation, development of CZE coupled with MS detection has been limited. Recently, we published several research papers on bottom-up characterization of mAbs and biosimilars highlighting the potential of CZE-electrospray ionization (ESI)-MS to obtain full primary structure and microvariant characterization as well as biosimilarity assessment.<sup>12–14</sup> However, in the bottom-up approach, BGE is totally compatible with ESI-MS, whereas for an intact MW or a middle-up approach, BGE involves a high concentration in nonvolatile salt or detergent which precludes the use of ESI-MS.<sup>20–22</sup> To our knowledge, some groups defined CZE-UV conditions for the separation of intact mAbs to always involve high levels of  $\epsilon$ -amino-caproic acid (EACA) and the addition of triethylenetetramine (TETA) or Tween 20.<sup>23–27</sup> Despite very interesting results in the separation of charge variants, BGEs are totally incompatible with ESI-MS.<sup>28</sup> In 2014, we developed the first analysis of intact mAb charge variant by CZE using a matrix-assisted laser desorption/ionization-MS (MALDI) detection.<sup>29–31</sup> Unfortunately, the limitation of

MALDI-MS resolution is that it does not allow one to measure the exact mass of the charge variants. More recently, Redman et al. published an important paper on the first characterization of intact mAb variants using microfluidic CZE-ESI devices.<sup>28</sup>

In this work, we developed a strategy to perform off-line CZE-UV/ESI-MS with the use of CZE-UV/fraction collection technology to perform CZE separation, followed by ESI-MS infusion of the different fractions using the capillary electrophoresis-electrospray ionization (CESI) interface as the nanoESI platform. Hydroxypropylcellulose (HPC) coating was used to minimize analyte adsorption on the capillary wall and reduce electroosmotic mobility (EOF). As one of the aims is to be compatible with ESI-MS, asymmetric CZE conditions bringing into play different BGE at the ends of the capillary have been developed. Inlet BGE composed of  $\epsilon$ -amino-caproic acid (EACA; 200 mM) and ammonium acetate (25 mM, pH 5.70) allowed one to conserve performance of CZE separation while outlet BGE composed only of ammonium acetate (25 mM) allowed for compatibility with ESI-MS. On the basis of the work of Gahoual et al., we used the CESI interface as the nanoESI infusion platform to allow us to generate a stable spray at 100 nL/min with sample consumption of 2  $\mu$ L per fraction to avoid the dilution effect.<sup>32</sup> The mAb selected was Cetuximab which is human/murine chimeric IgG-1 directed against the epidermal growth factor receptor (EGFR) overexpressed in advanced-stage EGFR positive colorectal cancer.<sup>33</sup> Cetuximab was approved in the US and EU in 2004 and 2005, respectively, and will be off-patent soon. Cetuximab contains two sites of glycosylation on the HC: one is located in the Fc/2 domain (Asn<sup>299</sup>) and the second is located in the F(ab')<sub>2</sub> domain on Asn<sup>88</sup> (Figure 1). It is an ideal sample for the evaluation of our strategy by the middle-up approach. Indeed, Cetuximab subunits

characterization allowed us to locate and to identify glycoforms. The performance of our strategy is demonstrated by the characterization of C-terminal lysine variants and the first separation of glycoforms of Cetuximab subunits using CZE-UV off-line hyphenated to ESI-MS after fraction collection.

## EXPERIMENTAL SECTION

**Materials.** Methanol (HPLC gradient grade) and acetic acid (100%) were obtained from VWR (Radnor, PA, USA). Ammonium acetate (>98%), sodium hydroxide, *ε*-amino-caproic acid (>98%), hydroxypropylcellulose (HPC;  $M_w$  100 000), and formic acid (>98%) were purchased from Sigma-Aldrich (Saint Louis, MO, USA). Water used to prepare buffers and sample solutions was obtained using an ELGA purelab UHQ PS water purification system (Bucks, UK). IdeS (immunoglobulin-degrading enzyme of *Streptococcus pyogenes*) also named FabRICATOR was purchased from Genovis (Lund, Sweden). Cetuximab (Erbitux, Merck KGaA, Darmstadt, Germany) is a sterile, preservative-free solution for intravenous infusion containing 5 mg/mL Cetuximab. The other ingredients are sodium chloride, glycine, polysorbate 80, citric acid monohydrate, sodium hydroxide, and water for injections.

**Middle-up Sample Preparation.** Cetuximab was cleaved in the hinge region using limited proteolysis by IdeS (FabRICATOR, Genovis) to obtain two Fc/2 fragments (calculated pI of 7.74) and one F(ab')<sub>2</sub> fragment (calculated pI of 7.78) (Figure 1). Sample was diluted using 147.25  $\mu$ L of 50 mM sodium phosphate, 150 mM NaCl, pH 6.60, to a final concentration of 1  $\mu$ g/ $\mu$ L. A volume of 2.25  $\mu$ L of IdeS (67 units/ $\mu$ L) was added to the sample which was left at 37 °C for 30 min. After digestion completion, sample was desalted using Amicon centrifugal filters (cut off = 10 000 Da) in pure water at 10 °C and 14 000g for 20 min. After the desalting step, sample volume was reduced to around 10  $\mu$ L. Sample was finally diluted to an assumed final concentration of 5  $\mu$ g/ $\mu$ L in a total volume of 30  $\mu$ L of pure water.

**Capillary Electrophoresis.** The CZE experiments were carried out on a P/ACE MDQ CE system from Sciex Separation (Brea, CA) equipped with a UV detection, a temperature controlled autosampler, and a power supply able to deliver up to 30 kV. A 32 Karat 8.0 (Sciex Separation, Brea, CA) was used for instrument control, data acquisition, and data handling. Polymicro bare fused-silica capillaries of 75  $\mu$ m i.d., 375 o.d. (75.5 cm effective length, 82 cm total length) were obtained from Photonlines (St-Germain-en-Laye, France). New capillaries were conditioned by successive flushes with 1.00 and 0.10 M NaOH and then with water under a pressure of 30 psi for 10 min each. The temperature in the capillary cartridge and autosampler were set at 25 °C. The acquisition rate was 10 points/s. Capillaries were rinsed with water and dried by air when not in use. UV absorbance was fixed at 200 nm. Voltage was applied at 20 kV with a ramp of 0.17, and injection sample condition was 0.5 psi for 50 s. Concerning modified capillaries, capillaries were coated in the laboratory with hydroxypropylcellulose (HPC;  $M_w$  100 000) following the protocol described by Shen and Smith.<sup>34</sup> 5% HPC in pure water (w/v) was prepared to perform capillary coating. Durability of coating is around 20 runs without a recoating step. For Cetuximab separation, inlet BGE 200 mM *ε*-amino-caproic acid (EACA)-ammonium acetate (25 mM, pH 5.70) and outlet BGE ammonium acetate (25 mM, pH 5.70) have been used as the separation condition. Injection volumes have been calculated using CEToolbox application (Pansanel, GooglePlay).

**CZE/Collection Fraction Interface.** This interface is described in a previous study.<sup>31</sup> Briefly, automated off-line coupling of CZE to MS was performed by using a homemade modified automatic spotting device Proteiner FC (Bruker Daltonics, Bremen, Germany) for the sheath flow-assisted spotting from the CZE capillary end onto a fraction collection target. The original setup of the UV cell in the P/ACE MDQ (Sciex Separation, Brea, CA) was modified in order to allow the simultaneous UV detection and fraction collection. Hystar 3.2 (Bruker Daltonics, Bremen, Germany) was used for Proteiner FC control.

**CESI as NanoESI Infusion Platform.** The infusion experiments were carried out with a PA 800 plus capillary electrophoresis (CE) system from Sciex Separation (Brea, CA) equipped with a temperature controlled autosampler and a power supply able to deliver up to 30 kV. Prototype fused-silica capillaries (total length of 95 cm; 30  $\mu$ m i.d.) whose outlet end (about 3 cm) was etched with hydrofluoric acid were used for all related CESI experiments and initially provided by Sciex Separation (Brea, CA, USA). It is certainly noteworthy to mention here that the inner lumen of these capillaries is not tapered and presents an i.d. of 30  $\mu$ m throughout its entire length. New capillaries were initially conditioned by flushing them for 10 min with MeOH, 10 min with 0.10 M sodium hydroxide, 10 min with 0.10 M hydrochloric acid, and finally with water for 20 min, each flushing step being conducted at 75 psi (5.17 bar).

**MALDI-TOF-MS.** The matrix was prepared by dissolving 2,5-dihydroxybenzoic acid (DHB; 2 g/L) in 0.1% trifluoroacetic acid/acetonitrile (TFA/ACN; 30/70, v/v). Fraction collection was realized using Ground Steel MALDI target (Bruker Daltonics, Bremen, Germany). Mass spectra of the CZE fractions were recorded using an Autoflex II MALDI-TOF (Bruker Daltonics, Bremen, Germany), operating in reflector mode and with FlexControl software. Positively charged ions were detected, and sums of 1500 single-shot spectra were acquired automatically from each sample by using the AutoXecute software. Data processing was performed with FlexAnalysis 3.0 provided by the mass spectrometer manufacturer. All spectra were calibrated according an external calibration using Protein calibration standard I (Bruker Daltonics, Bremen, Germany) for intact protein separation.

**ESI-TOF-MS.** For sheathless CZE-ESI-MS experiments, the CE system was coupled to a maxis 4G (Bruker Daltonics, Bremen, Germany). MS transfer parameters were optimized using the actual sample directly infused via the CE system using a pressure of 5 psi (340 mbar). MS parameters were optimized so that high  $m/z$  ions could be properly transferred to the TOF analyzer while avoiding fragmentation. In the case of the maxis 4G, ion funnels were set at values of 300 and 400 Vpp. The electrospray voltage (capillary voltage) typically ranged from -1.2 to -1.8 kV. Dry gas was set at 1.5 L/min and source temperature at 180 °C. Data processing was performed with DataAnalysis 4.0. Deconvolution of the mass spectra was performed on the basis of maximum entropy analysis using ESI Compass 1.3 Maximum Entropy Deconvolution Option in DataAnalysis 4.0. All spectra were calibrated by external calibration using Pepmix (Bruker Daltonics, Bremen, Germany) and CsI from Sigma-Aldrich (Saint-Louis, MO, USA).

## RESULTS AND DISCUSSION

**Optimization of CZE Separation Conditions.** As the aim is to develop a procedure for the middle-up characterization of Cetuximab using the potential of the CZE separation method and suitable for ESI-MS direct infusion, we have optimized BGEs

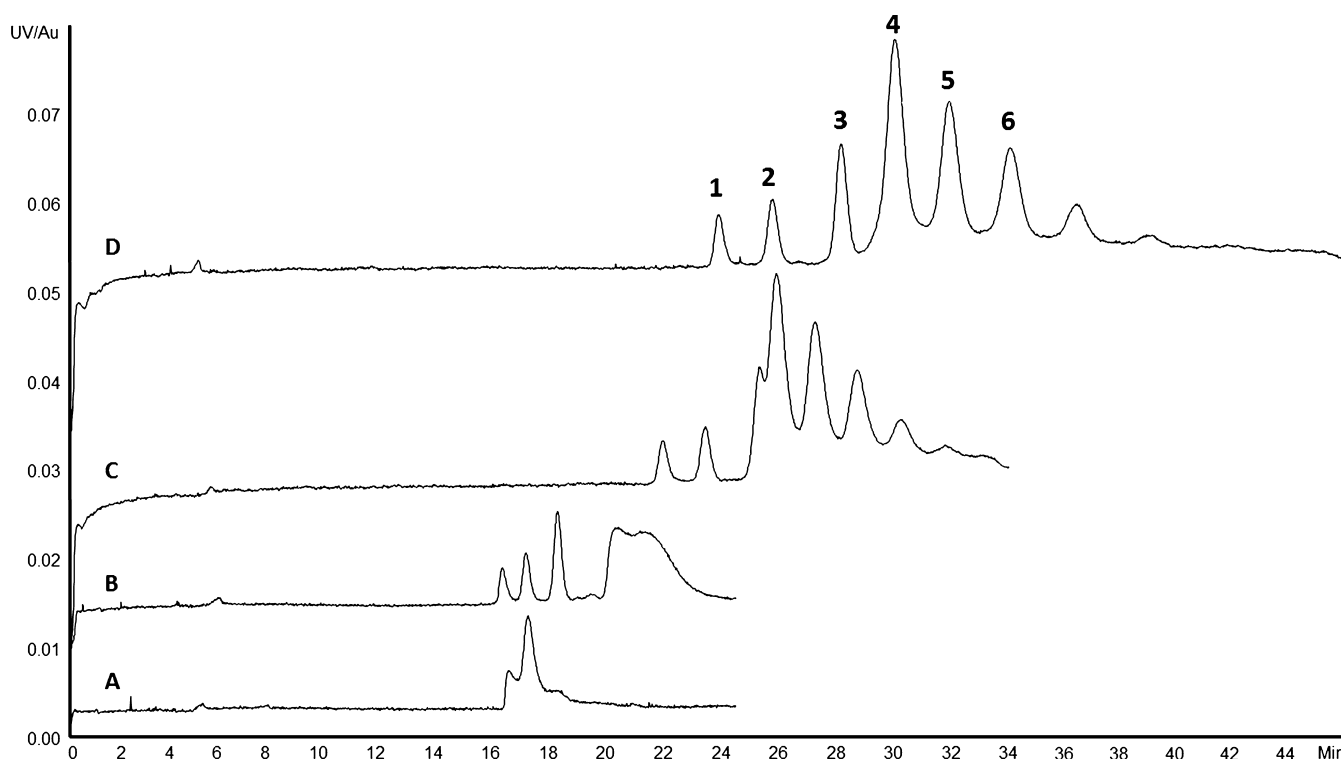


**Figure 2.** Impact of ammonium acetate concentration in BGE on electrophoretic resolution. BGE composed of a mixture of EACA (200 mM) and acetate ammonium (A) 5 mM, (B) 10 mM, (C) 25 mM, and (D) 50 mM, at pH 5.70. Peaks 1–3 correspond to Fc/2 variants, and peaks 4–6 correspond to F(ab')<sub>2</sub> variants. Experimental conditions: HPC-coated capillary; total/effective length of 82/75.5 cm × 75 μm i.d.; voltage, 20 kV; UV absorbance at 200 nm; sample, IdeS digest of Cetuximab (5 μg/μL); sample injection; 0.5 psi for 50 s.

as mixtures of components that facilitate isoforms separation and allow the use of the ESI ionization process. First, we based our research on the study developed by the group of Pr. Somsen on the glycoform profiling of interferon-β-1a and erythropoietin.<sup>19</sup> However, using the condition based on the HPC coated capillary and 50 mM acid BGE, no separation of Cetuximab isoforms had been obtained. To our knowledge, some groups defined CZE-UV conditions for the separation of intact mAbs to always involve high levels of EACA and the addition of TETA or Tween 20.<sup>23–27</sup> EACA is a zwitterion which can be used to create high ionic strength and low conductivity buffers that minimize the electroosmotic flow (EOF) and improve electrophoretic mobility differences. TETA and Tween 20 behave as a modifier in BGE for dynamic coating to reduce or prevent analyte adsorption in the capillary wall.<sup>35–37</sup> Despite very interesting results in the separation of charge variants due to the presence of these modifiers, the major issue of these BGE conditions is the incompatibility with ESI-MS detection. The first step of our optimization consisted of eliminating Tween 20 and TETA in the BGE. Indeed, following the results described by Gassner et al., we minimize analyte adsorption only by the use of a HPC coating.<sup>25</sup> This allows one to remove the use of additional detergent or oligoamine, and it additionally presents the advantage of being a static coating that avoids potential polymer release for ESI-MS infusion. In a previous work, we demonstrated the high repeatability and the good robustness obtained with HPC-coated capillary for the separation of intact mAbs (RSD < 0.5%, migration time).<sup>31</sup> The second step of our BGE screening concerned the use of a high level of EACA. He et al. demonstrated the influence of pH and EACA concentration on the mAb separation.<sup>23</sup> Concerning EACA concentration, they demonstrated that increasing EACA concentration may improve

separation efficiency and electrophoretic resolution. However, due to zwitterionic properties, EACA based BGE involves significant interference with the sample in the ionization process of ESI-MS. Despite this, the presence of EACA in the BGE remains essential to maintain the separation efficiency particularly due to the low conductivity. On the basis of the results of Ruesch's team<sup>23</sup> and some difficulties of matrix/sample crystallization for the MALDI-MS experiment observed in previous study, we decided to reduce the EACA concentration from 400 to 200 mM and to add ammonium acetate at a pH of 5.70. Ammonium acetate is usually employed with ESI-MS mainly for volatility properties of the ammonium ion and good compatibility with the process of ionization. To perform separation, we used our homemade CZE-UV/fraction collection described in a previous work.<sup>31</sup> BGEs are placed in the inlet and outlet vials of the CE apparatus. Due to the modification of the CE cartridge, outlet BGE has been used as the sheath liquid with a flow rate of 0.5 μL/min. Fraction collection was directly deposited on a target plate. Each peak is collected on the basis of its apparent mobility described by the equation:

$$\mu_{\text{app}} = \frac{Ll}{t_m V}$$

with  $\mu_{\text{app}}$  being the apparent mobility, which is the sum of effective mobility and residual EOF,  $L$  and  $l$  being the total capillary length and length to the detection window, respectively,  $V$  being the applied voltage, and  $t_m$  being the migration time. Deposition time  $t_d$  is then calculated by the equation:

$$t_d = \frac{L^2}{\mu_{\text{app}} V}$$

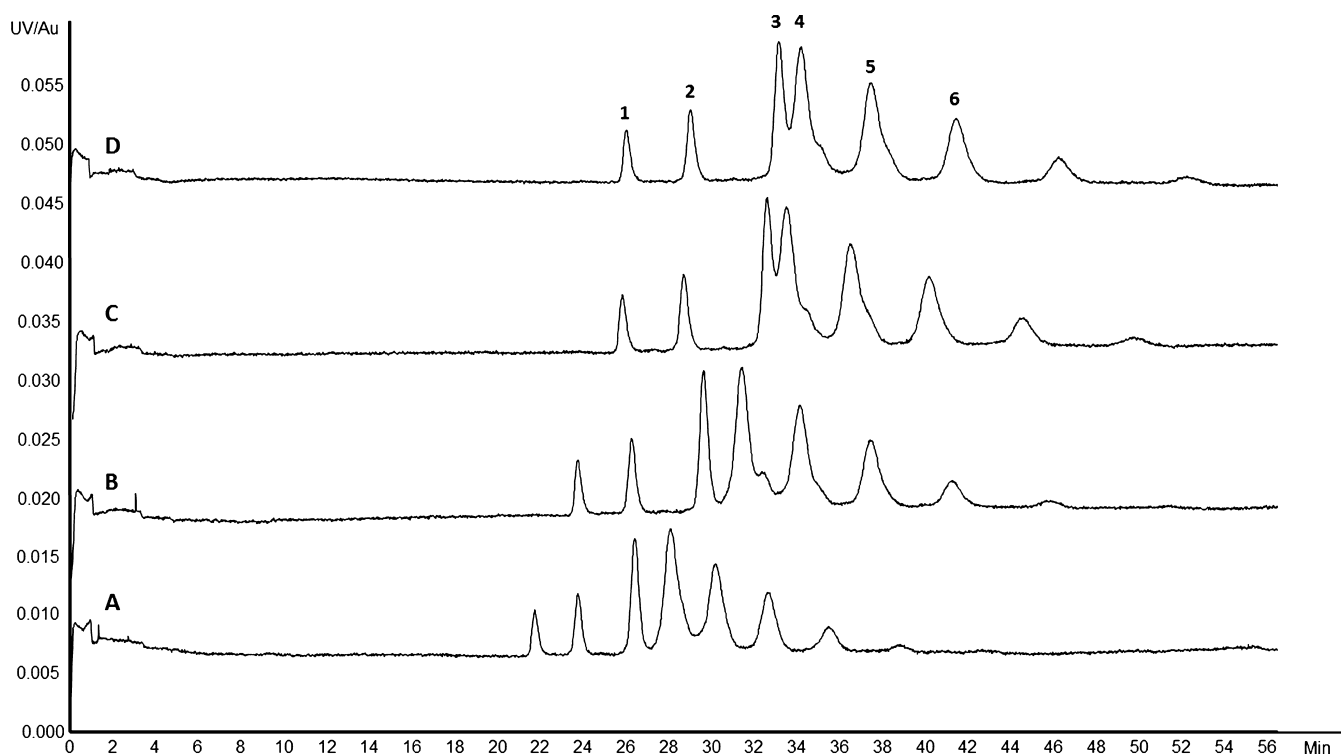


**Figure 3.** Impact of ammonium acetate concentration in outlet BGE on electrophoretic resolution. Inlet BGE composed of a mixture of EACA (200 mM) and acetate ammonium (25 mM, pH 5.70) and outlet BGE by ammonium acetate (A) 12.5 mM, (B) 25 mM, (C) 50 mM, and (D) 100 mM, at pH 5.70. Peaks 1–3 correspond to Fc/2 variants and peaks 4–6 correspond to F(ab')<sub>2</sub> variants. Experimental conditions: HPC-coated capillary; total/effective length, 82/75.5 cm × 75 μm i.d.; voltage, 20 kV; UV absorbance at 200 nm; sample injection, 0.5 psi for 50 s.

The results presented in Figure 2 show the CZE-UV separation of Cetuximab IdeS fragments (Figure 1) with different BGEs at pH 5.70 composed of the mixture of EACA (200 mM) and various concentrations of ammonium acetate (from 5 to 50 mM). Electropherograms presented in Figure 2 show a drastic decrease of electrophoretic resolution with the lowest concentration of ammonium acetate until complete loss of separation with 5 mM ammonium acetate (electropherogram A). These results confirm the trend in loss of electrophoretic resolution with the decrease of the ionic strength. Electropherogram D corresponding to BGE composed of EACA (200 mM) and ammonium acetate (50 mM, pH 5.70) shows the best separation with electrophoretic resolution up to 1.63 for peaks 1–3 corresponding to Fc/2 variants and an average electrophoretic resolution of 1.02 for peaks 4–6 corresponding to F(ab')<sub>2</sub> variants.

However, outlet BGE, which plays the role of sheath liquid, is composed of 200 mM EACA which can compromise the ESI-MS ionization process. Indeed, to verify the impact of the presence of EACA in the BGE, we obtain MALDI-MS mass spectra of the different fractions corresponding to the six major peaks. No signals were observed by MALDI-MS because of the lack of crystallization of the sample with the DHB matrix (Figure S-1 part A, Supporting Information). The presence of EACA in the BGE gives a white homogeneous deposit totally different from the spangled classical one. MALDI-MS detection failure and the experimental ESI-MS infusion of fraction 3 without any MS signal (data not shown) allows us to conclude that direct ESI-MS infusion is completely impossible in these conditions.

On the basis of the CZE-ESI-MS sheath liquid interface described by the group of Smith<sup>38</sup> and the fact that the additional liquid is usually different from the BGE composition, we decided

to develop asymmetric conditions between the inlet BGE and the outlet BGE. As the aim of the study is to conserve the electrophoretic resolution of the separation, to allow ESI-MS detection and to avoid the Joule heating effect, inlet BGE has been chosen as EACA (200 mM) and ammonium acetate (25 mM, pH 5.70). A different BGE, placed in the outlet vial, is composed only with ammonium acetate at pH 5.70.

To optimize the separation, different concentrations of ammonium acetate from 12.5 to 100 mM have been tested as outlet BGE. Results are presented in Figure 3. Electropherograms C and D show a loss of electrophoretic resolution between peak 3 and peak 4 corresponding to the last peak of Fc/2 variants and the first peak of F(ab')<sub>2</sub> variants. Electropherogram B, corresponding to outlet BGE composed of ammonium acetate (25 mM, pH 5.70), shows the best separation with electrophoretic resolution up to 2.10 for peaks 1–3 corresponding to Fc/2 variants and an average electrophoretic resolution of 1.05 for peaks 4–6 corresponding to F(ab')<sub>2</sub> variants. These results show no loss of electrophoretic resolution using electropherogram B conditions as compared to Figure 2 experiments. This demonstrates that the presence of a high concentration of EACA in the outlet BGE is not necessary to achieve the separation. As the aim was to verify the impact of the absence of EACA in the outlet BGE, we performed a MALDI-MS detection of the different fractions corresponding to the six major peaks. First of all, we observed a good crystallization of sample with the DHB matrix (Figure S-1 part B, Supporting Information) which confirms no contamination of EACA during the deposit process. Figure 4 emphasizes the mass spectrum of each peak. Moreover, the CZE-MALDI-MS (Figure 4b) confirms the good agreement between the UV detection and the deposition time in terms of Fc/2 and F(ab')<sub>2</sub> separation. This also confirms the absence of

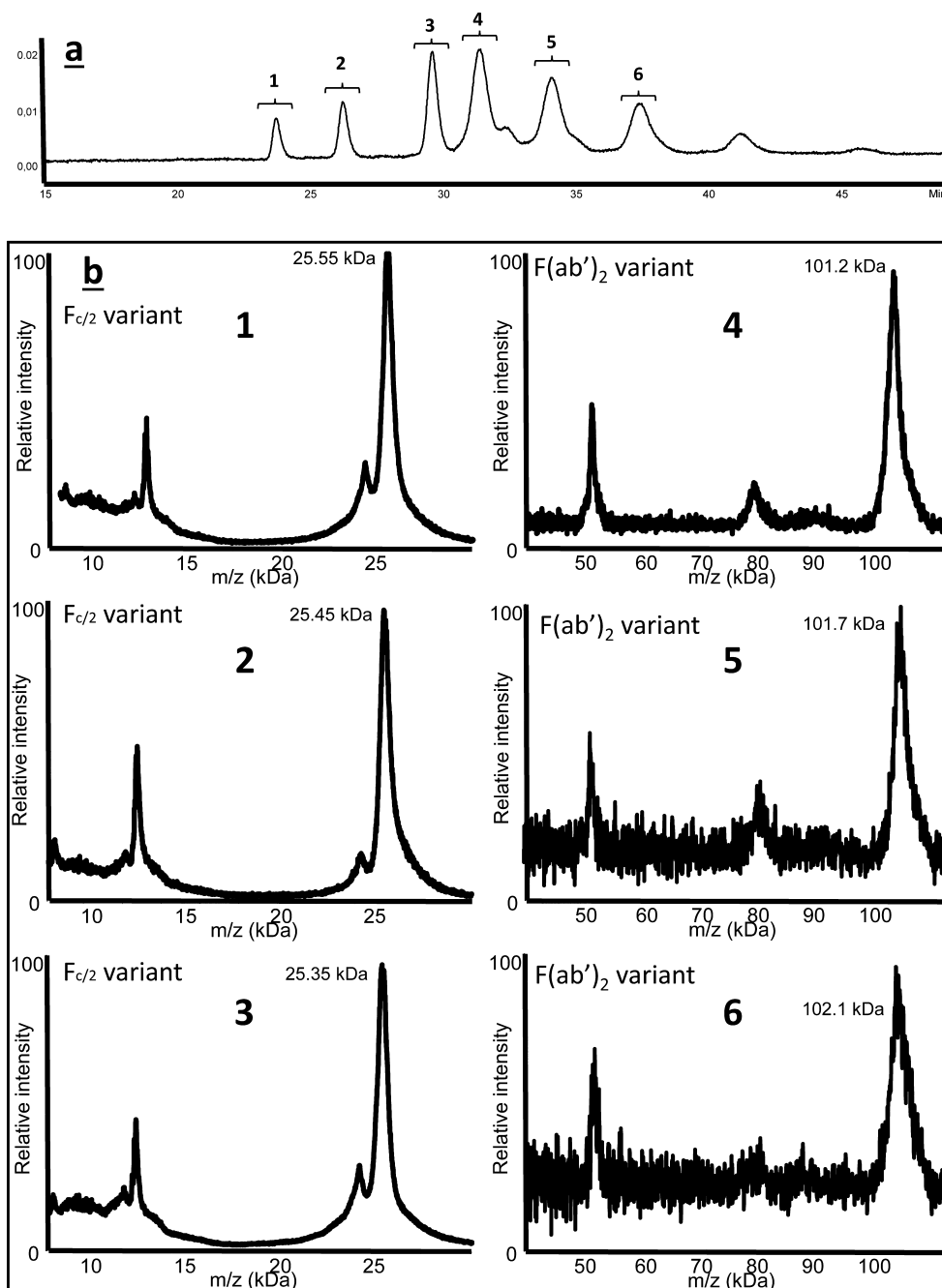


**Figure 4.** CZE-UV off-line coupled to MALDI-MS via fractionation for a middle-up characterization of Cetuximab charge variants. (a) CZE-UV electropherogram. (b) Analysis of CZE-UV fractions by MALDI-MS. Mass spectra of the six major peaks. CE experimental conditions: Inlet BGE: EACA (200 mM) and acetate ammonium (25 mM, pH 5.70); outlet BGE: ammonium acetate (25 mM, pH 5.70); other conditions: see Figure 2. MS experimental conditions: see Experimental Section; sample, IdeS digest of Cetuximab (5  $\mu\text{g}/\mu\text{L}$ ); sample injection, 0.5 psi for 50 s.

carryover effect and the diffusion phenomenon. Unfortunately, the limitation of MALDI-MS resolution for molecules up to 20 kDa does not allow one to measure the exact mass of the charge variants and then to thoroughly characterize these glycoproteins. Thus, to reach higher MS resolution at comparable separation efficiency, we switched to ESI-MS detection using CESI as the nanoESI infusion platform. This strategy of collection fraction followed by nanoESI infusion opens the way for a deeper characterization of  $\text{Fc}/2$  and  $\text{F}(\text{ab}')_2$  domains without sample treatment and with minimum sample volume (2  $\mu\text{L}$ ).

**Middle-up Characterization of Cetuximab.** Cetuximab is a chimeric mouse-human IgG1 known to bear 2 N-glycosylation

sites on each heavy chain (HC).<sup>11</sup> Moreover, Cetuximab has a large number of microheterogeneities such as PTMs including methionine oxidation, asparagine deamidation, or isomerization of aspartic acid. Furthermore, this mAb also has one C-terminal lysine truncation. These features make Cetuximab an ideal sample for the evaluation of a middle-up approach using CE-MS coupling. In order to simplify the location of N-glycosylation, IdeS enzymatic reaction (Figure 1) cleaves Cetuximab in the middle of HC to obtain two types of fragments each carrying one N-glycosylation site. Direct ESI-MS infusion of IdeS fragments of Cetuximab proved to have equal signal abundances for C-terminal lysine variants, which involve two distinct profiles for

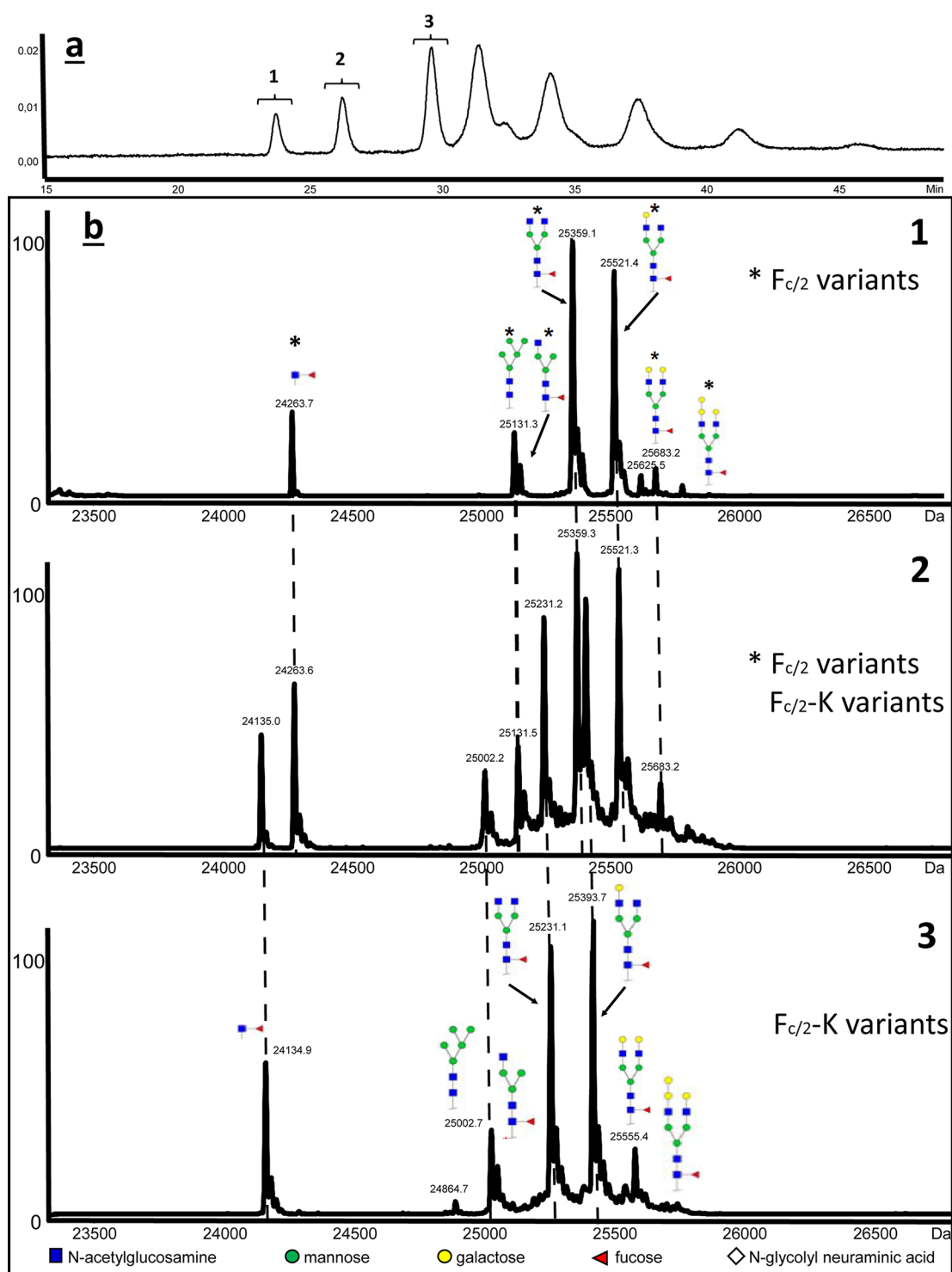


**Figure 5.** (a) Off-line CZE-UV/ESI-MS separation of middle-up Cetuximab charge variants. (b) Deconvoluted mass spectra for each Fc/2 variant. The MS peaks were labeled with the correspondent glycoform. Experimental conditions: Inlet BGE: EACA (200 mM) and ammonium acetate (25 mM, pH 5.70); outlet BGE: ammonium acetate (25 mM, pH 5.70); other conditions: see Figure 2. MS Experimental conditions: see Experimental Section; sample, IdeS digest of Cetuximab (5  $\mu\text{g}/\mu\text{L}$ ); sample injection, 0.5 psi for 50 s.

the Fc/2 domains and a complex glycoprofiling for the F(ab')<sub>2</sub> domain (Figure S-2, Supporting Information). With this knowledge, we can expect to observe a few peaks corresponding to Fc/2 fragments due to a loss of a +1 charge associated with C-terminal lysine truncation. In addition, we also expect a few peaks for F(ab')<sub>2</sub> fragments because of the ability of CZE to resolve glycoforms with acidic glycans, due to a reduction in net

charge by addition of negatively charged sialic acid compound. Preliminary MALDI-MS results presented in Figure 4 confirmed these predictions with peaks 1–3 corresponding to Fc/2 fragments and at least peaks 4–6 corresponding to F(ab')<sub>2</sub> fragments.

To enhance MS resolution, the same experiment was performed to collect fractions of each peak and to analyze them by

nanoESI-MS using the CESI interface as the infusion platform. After deposition, each fraction was collected and evaporated. No special treatment was made for the collected fractions. Before infusion, dry samples were reconstituted in 2  $\mu$ L of 50%/49%/1% acetonitrile/water/formic acid (v/v/v) in order to enhance sample ionization. Thus, each fraction was infused into the MS using a flow rate of 100 nL/min in order to enhance sensitivity. The total volume of sample infused to perform one acquisition was about 600 nL which represents a 100 times reduction in terms of sample consumption as compared to standard ESI-MS. This point is critical as the volume of each fraction does not expect a few  $\mu$ L to avoid the dilution effect.

Deconvoluted charge variant mass spectrum of fractions from peak 1 to peak 3 generated multiple masses corresponding to the expected presence of neutral glycosylation variants of Fc/2 fragments (Figure 5). In addition, the comparison with the direct infusion experiment (Figure S-2, Supporting Information) showed us that the two Fc/2 fragments, corresponding to one intact and one with lysine truncation, are detected and separated. Deconvoluted mass spectra corresponding to peak 1 and peak 3 show a difference of 128 Da between the mass peak at 25 359.1 Da corresponding to the most abundant Fc/2 glycoform (G0F) and the mass peak at 25 231.1 Da corresponding to G0F for Fc/2-K. Thus, we obtained the complete separation of these two fragments (Figure 5b-1 and -3). In agreement with Ayoub et al.<sup>11</sup> and with the comparison of direct infusion of Cetuximab IdeS subunits (Figure S-2, Supporting Information), only one possibility of C-terminal lysine loss was expected. Regarding deconvoluted mass spectra of peak 2, it shows a nearly equal abundance mixture of Fc/2 and Fc/2-K variants. These peaks deconvolute to the same MWs found in peak 1 and peak 3 and could be interpreted by an overlap during the deposit process. However, regarding the MS signal of raw data used to generate deconvoluted spectra of peak 1, peak 2, and peak 3 and considering a potential equivalent ionization efficiency of all Fc/2 variants, the intensity of peak 2 is higher than that of peak 1 and less than that of peak 3 (Figure S-3, Supporting Information) following the CZE separation pattern. This observation should eliminate a potential carryover effect (peak broadening, excessive diffusion) which should show a concomitant decrease of peak 1 MS intensity and increase of peak 2 MS intensity. In addition, to exclude carryover effect, we performed infusion of fractions corresponding to peak 4 and to a period of 2 min before detection of peak 1. No ESI-MS spectra have been detected corresponding to Fc/2 fragment (data not shown). Cetuximab, as other mAbs, is known to have a large number of micro-heterogeneities commonly found in proteins which are reflected by differences in mass, charge, or conformation and then differences in effective mobilities. Moreover, it is plausible that several cumulative modifications could lead to a variation of conformation without mass shifts, although further work is required to identify these modifications.

An important class of modification that can significantly impact the immunogenic properties of Cetuximab in terms of PK and PD is glycosylation.<sup>10</sup> Cetuximab contains two sites of glycosylation on the HC: one is located in the Fc/2 domain (Asn<sup>299</sup>) and the second is located in the F(ab')<sub>2</sub> domain on Asn<sup>88</sup>.<sup>7</sup> Cetuximab has been widely described in terms of glycan characterization.<sup>4,39</sup> In 2013, Janin-Bussat et al. used a middle-up approach, similar to the one described here but using the HPLC-MS method, and identified 17 different glycoforms distributed on the two glycosylation sites.<sup>40</sup> In 2013, Dr. Beck's team characterized 24 different glycosylations using a combination of

intact, middle-up, middle-down, and bottom-up ESI and MALDI-MS techniques.<sup>11</sup> More recently, Gahoual et al. characterized 15 glycopeptides using a bottom-up approach by CESI-MS/MS.<sup>13</sup> In our work, we could identify a total of 15 glycans divided between 7 for the Fc/2 N-glycosylation and 8 for the F(ab')<sub>2</sub> N-glycosylation (Tables S-1 and S-2, Supporting Information). Regarding the Fc/2 domain, branched glycan structures are primarily composed of fucose, N-acetylglucosamine, and mannose but can differ in the number of terminal galactose, mannose, or N-acetylglucosamine residues. Glycan structure with the addition of galactose moieties involves a mass increase of 162 Da but does not induce a change in net charge.<sup>41,42</sup> Gahoual and co-workers demonstrated that particular glycopeptides having a difference of one galactose could be baseline separated<sup>13</sup> whereas Redman et al. did not observe mobility shifts between intact mAb glycoforms due to the low impact of 162 Da on the mass of intact mAb ( $\approx 0.1\%$ ).<sup>28</sup> Our work demonstrated that, concerning glycoform with a difference of one galactose residue, the middle-up approach does not allow one to observe baseline separations. The mass of galactose moiety accounts for  $\approx 0.6\%$  of the Fc/2 domain and  $\approx 0.2\%$  of the F(ab')<sub>2</sub> domain. Following the conclusion of Redman et al.,<sup>28</sup> to induce effective mobility shift, the mass increase would have to be much greater or induce a significant change in conformation. However, CE has the potential to separate glycoforms bearing acidic residues, due to a reduction in net charge from the addition of negatively charged sialic acid.<sup>41</sup> Due to this, Cetuximab appears to be an ideal sample.

Indeed, regarding the F(ab')<sub>2</sub> domain, Ayoub et al.<sup>11</sup> identified glycosylations with 41% glycans bearing N-glycolyl neuraminic acid (NGNA) in their structures. NGNA glycoforms result from the SP2/0 murine expression system used to produce Cetuximab.<sup>43</sup> When produced in CHO cells, the biobetter version exhibits N-acetylneuraminic acid (NANA) glycoforms.<sup>9</sup> Despite the high proportion of the NGNA glycan, no separation of F(ab')<sub>2</sub> variants was obtained using HPLC-MS.<sup>11</sup> As shown in Figure 6, electrophoretic peaks from 4 to 6 correspond to different F(ab')<sub>2</sub> variants. Deconvolution of each charge variant mass spectrum generated multiple masses, corresponding for peak 4 to the expected presence of neutral glycosylation variants. Following the theory developed previously for the Fc/2 variants, neutral residues did not allow effective mobility shift of F(ab')<sub>2</sub> glycoforms due to the small impact of galactose mass residue in the F(ab')<sub>2</sub> mass. The mass ascribed to the most intense mass peak of 101 924 Da (Figure 6b-4) corresponds to the most abundant F(ab')<sub>2</sub> glycoform (G2FGal2/G2FGal2). Four other less abundant F(ab')<sub>2</sub> glycoforms are labeled, each one bearing galactose residues (Figure 6b-4). Deconvoluted mass spectra presented in Figure 6b-5 correspond to the F(ab')<sub>2</sub> glycoforms contained in peak 5. In this fraction, the most abundant mass peak of 102 069 Da presents a mass difference of 145 Da compared to GF2Gal2/GF2Gal2 which corresponds to the presence of a NGNA residue instead of a galactose residue. This mass peak corresponds to the second most abundant F(ab')<sub>2</sub> glycoform (GF2Gal2/GF2Gal2NGNA). Another mass peak at 102 592 Da has been labeled in the mass spectra. This corresponds to a less abundant F(ab')<sub>2</sub> glycoform also bearing one NGNA residue in the glycan structure. We note that common mass peaks are detected in fractions 4 and 5. Indeed, the electrophoretic resolution of 1.05 does not allow the complete separation; however, we observe an important decrease of intensity for the glycoforms detected in fraction 4. Finally, the infusion of fraction 6, corresponding to the sixth peak of the



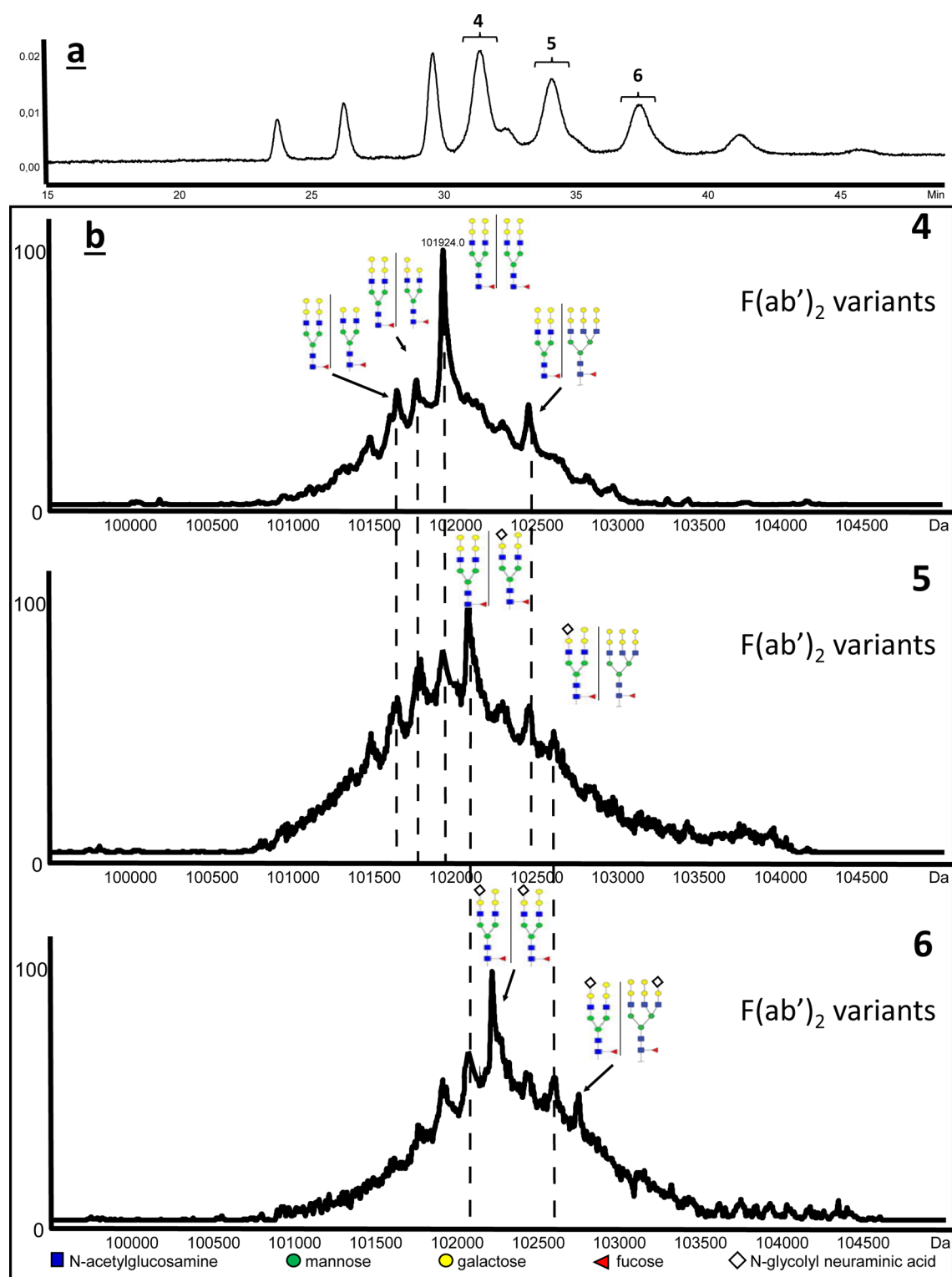


**Figure 6.** (a) Off-line CZE-UV/ESI-MS separation of middle-up Cetuximab charge variants. (b) Deconvoluted mass spectra for each F(ab')<sub>2</sub> variant. The MS peaks were labeled with the correspondent glycoform. Experimental conditions: Inlet BGE: EACA (200 mM) and ammonium acetate (25 mM, pH 5.70); outlet BGE: ammonium acetate (25 mM, pH 5.70); other conditions: see Figure 2. MS Experimental conditions: see Experimental Section; sample, IdeS digest of Cetuximab (5 μg/μL); sample injection, 0.5 psi for 50 s.

electrophoretic separation (Figure 6b-6), gives deconvoluted mass spectra corresponding to F(ab')<sub>2</sub> glycoforms with the combination of glycan structures each bearing one NGNA residue (GF2GalNGNA/GF2GalNGNA). Indeed, the most intense peak showing a deconvoluted mass of 102 217 Da also

presents a difference of 145 Da compared to GF2GalNGNA/GF2GalNGNA which corresponds to the presence of a second NGNA residue instead of a galactose residue. Moreover, as in fraction 5, another mass peak at 102 741 Da has been detected and corresponds to less abundant F(ab')<sub>2</sub> glycoforms also each

bearing one NGNA residue in the glycan structures. To our knowledge, these results represent the first separation of F(ab')<sub>2</sub> glycoforms using CZE-MS coupling. Since it is known that these glycosylations have been shown to be responsible for immunogenic responses,<sup>10</sup> separation of these glycoforms can be very helpful for the characterization of Cetuximab especially to highlight batch-to-batch variations in the glycosylation profiles or for biosimilarity assessment. Furthermore, no similar results have been described using HPLC-MS coupling. This highlights the potential of CZE separation to perform the middle-up approach of mAbs especially when they carry capping sialic acid carbohydrates.

## CONCLUSION

To summarize, we have reported an original strategy bringing into play an off-line CZE-UV/fraction collection method followed by nanoESI-MS infusion for the characterization of a therapeutic mAb. In order to realize mAb charge variants separation and to perform nano-ESI-MS detection, CZE conditions were optimized. First, to eliminate BGE additives, a HPC coated capillary was utilized to obtain residual EOF and to minimize analyte adsorption. Second, as the aim is to conserve electrophoretic resolution and complete compatibility with ESI-MS, asymmetric CZE conditions involving different BGE at the ends of the capillary have been described. Inlet BGE has been chosen as a mixture of EACA (200 mM) and ammonium acetate (25 mM, pH 5.70) and outlet BGE was composed of only ammonium acetate (25 mM, pH 5.70). MWs were measured for six charge variants detected in the CZE separation of Cetuximab subunits through deconvolution of the mass spectra. The first three peaks correspond to Fc/2 variants, and the last three peaks correspond to F(ab')<sub>2</sub> variants. Separation performance obtained with these conditions showed electrophoretic resolution up to 2.10 for Fc/2 variants and an average electrophoretic resolution of 1.05 for F(ab')<sub>2</sub> variants. Regarding Fc/2 domain, two C-terminal lysine variants were identified and separated. Moreover, the separation of Fc/2 fragments allowed the glycoprofiling of the variants with the characterization of 7 glycoforms, each bearing neutral residues to the glycan structure. Regarding F(ab')<sub>2</sub> domain, deconvolution of the mass spectra allowed the determination of 8 glycoforms detected and separated in different peaks. Glycoforms separation is due to the presence of NGNA residues in some glycan structure. Four glycosylations of F(ab')<sub>2</sub> variants were identified by a characteristic 145 Da mass shift; moreover, this identification was supported by the decrease of effective mobility due to a reduction in net charge from the addition of negatively charged sialic acid. To our knowledge, this work represents the first demonstration of a middle-up approach of mAb using CZE-MS and in addition the first separation of F(ab')<sub>2</sub> glycoforms. This highlights the potential of CZE to perform separation of mAbs especially when they carry sialic acid groups. Moreover, the strategy of collection fraction followed by nanoESI infusion without sample treatment and in a sample volume of 2  $\mu$ L opens the way to different deeper characterization with, for example, a top-down approach using ESI-ETD-MS most likely unraveling additional information regarding the structure of the protein.

## ASSOCIATED CONTENT

### Supporting Information

Additional information about crystallization of matrix/sample in the presence or absence of EACA, direct ESI-MS infusion of Cetuximab, MS raw data of fraction 1–6, and theoretical

and measured masses of identified glycoforms as noted in the text. The Supporting Information is available free of charge on the ACS Publications website at DOI: 10.1021/acs.analchem.5b00928.

## AUTHOR INFORMATION

### Corresponding Author

\*E-mail: yfrancois@unistra.fr.

### Notes

The authors declare no competing financial interest.

## ACKNOWLEDGMENTS

The authors would like to thank Sciex separations Inc. for lending a CESI prototype and Dr. M. Anselme from Sciex separations Inc. for his support. The authors would like also to express their gratitude to Dr. E. Wagner-Rousset, Dr. D. Ayoub, M.-C. Janin-Bussat, and O. Colas (Centre d'Immunologie Pierre Fabre, St Julien en Genevois, France) for helpful discussions regarding antibody structural characterization.

## REFERENCES

- (1) Beck, A.; Wurch, T.; Bailly, C.; Corvaia, N. *Nat. Rev. Immunol.* **2010**, *10*, 345–352.
- (2) Reichert, J. M. *mAbs* **2012**, *4*, 413–415.
- (3) Arnold, J. N.; Wormald, M. R.; Sim, R. B.; Rudd, P. M.; Dwek, R. A. *Annu. Rev. Immunol.* **2007**, *25*, 21–50.
- (4) Zhang, Z. Q.; Pan, H.; Chen, X. Y. *Mass Spectrom Rev.* **2009**, *28*, 147–176.
- (5) McCamish, M.; Woollett, G. *Clin. Pharmacol. Ther.* **2013**, *93*, 315–317.
- (6) Beck, A.; Diemer, H.; Ayoub, D.; Debaene, F.; Wagner-Rousset, E.; Carapito, C.; Van Dorsselaer, A.; Sanglier-Cianferani, S. *TrAC, Trends Anal. Chem.* **2013**, *48*, 81–95.
- (7) Beck, A.; Sanglier-Cianferani, S.; Van Dorsselaer, A. *Anal. Chem.* **2012**, *84*, 4637–4646.
- (8) Beck, A.; Wagner-Rousset, E.; Ayoub, D.; Van Dorsselaer, A.; Sanglier-Cianferani, S. *Anal. Chem.* **2013**, *85*, 715–736.
- (9) Beck, A.; Debaene, F.; Diemer, H.; Wagner-Rousset, E.; Colas, O.; Dorsselaer, A. V.; Cianferani, S. *J. Mass Spectrom.* **2015**, *50*, 285–297.
- (10) Chung, C. H.; Mirakhor, B.; Chan, E.; Le, Q.; Berlin, J.; Morse, M.; Murphy, B. A.; Satinover, S. M.; Hosen, J.; Mauro, D.; Slebos, R. J.; Zhou, Q. W.; Gold, D.; Hatley, T.; Hicklin, D. J.; Platts-Mills, T. A. E. *New Eng. J. Med.* **2008**, *358*, 1109–1117.
- (11) Ayoub, D.; Jabs, W.; Resemann, A.; Evers, W.; Evans, C.; Main, L.; Baessmann, C.; Wagner-Rousset, E.; Suckau, D.; Beck, A. *mAbs* **2013**, *5*, 699–710.
- (12) Gahoual, R.; Burr, A.; Busnel, J. M.; Kuhn, L.; Hammann, P.; Beck, A.; Francois, Y. N.; Leize-Wagner, E. *mAbs* **2013**, *5*, 479–490.
- (13) Gahoual, R.; Busnel, J.-M.; Beck, A.; François, Y.-N.; Leize-Wagner, E. *Anal. Chem.* **2014**, *86*, 9074–9081.
- (14) Gahoual, R.; Biacchi, M.; Chicher, J.; Kuhn, L.; Hammann, P.; Beck, A.; Leize-Wagner, E.; Francois, Y. N. *mAbs* **2014**, *6*, 1464–1473.
- (15) Talebi, M.; Nordborg, A.; Gaspar, A.; Lacher, N. A.; Wang, Q.; He, X. Z. P.; Haddad, P. R.; Hilder, E. F. *J. Chromatogr. A* **2013**, *1317*, 148–154.
- (16) Mokaddem, M.; Gareil, P.; Varenne, A. *Electrophoresis* **2009**, *30*, 4040–4048.
- (17) Alvarez, M.; Tremintin, G.; Wang, J.; Eng, M.; Kao, Y.-H.; Jeong, J.; Ling, V. T.; Borisov, O. V. *Anal. Biochem.* **2011**, *419*, 17–25.
- (18) Haselberg, R.; Ratnayake, C. K.; de Jong, G. J.; Somsen, G. W. *J. Chromatogr. A* **2010**, *1217*, 7605–7611.
- (19) Haselberg, R.; de Jong, G. J.; Somsen, G. W. *Anal. Chem.* **2013**, *85*, 2289–2296.
- (20) Fekete, S.; Gassner, A. L.; Rudaz, S.; Schappeler, J.; Guilleme, D. *TrAC, Trends Anal. Chem.* **2013**, *42*, 74–83.
- (21) Farnan, D.; Moreno, G. T. *Anal. Chem.* **2009**, *81*, 8846–8857.

- (22) Rozhkova, A. J. *Chromatogr. A* **2009**, *1216*, 5989–5994.
- (23) He, Y.; Lacher, N. A.; Hou, W.; Wang, Q.; Isele, C.; Starkey, J.; Ruesch, M. *Anal. Chem.* **2010**, *82*, 3222–3230.
- (24) He, Y.; Isele, C.; Hou, W.; Ruesch, M. *J. Sep. Sci.* **2011**, *34*, 548–555.
- (25) Gassner, A. L.; Rudaz, S.; Schappler, J. *Electrophoresis* **2013**, *34*, 2718–2724.
- (26) Shi, Y.; Li, Z.; Qiao, Y. B.; Lin, J. *J. Chromatogr. B* **2012**, *906*, 63–68.
- (27) Espinosa-de la Garza, C. E.; Perdomo-Abundez, F. C.; Padilla-Calderon, J.; Uribe-Wiechers, J. M.; Perez, N. O.; Flores-Ortiz, L. F.; Medina-Rivero, E. *Electrophoresis* **2013**, *34*, 1133–1140.
- (28) Redman, E. A.; Batz, N. G.; Mellors, J. S.; Ramsey, J. M. *Anal. Chem.* **2015**, *87*, 2264–2272.
- (29) Amon, S.; Plematl, A.; Rizzi, A. *Electrophoresis* **2006**, *27*, 1209–1219.
- (30) Silvertand, L. H. H.; Toraño, J. S.; de Jong, G. J.; van Bennekom, W. P. *Electrophoresis* **2009**, *30*, 1828–1835.
- (31) Biacchi, M.; Bhajun, R.; Saïd, N.; Beck, A.; François, Y. N.; Leize-Wagner, E. *Electrophoresis* **2014**, *35*, 2986–2995.
- (32) Gahoual, R.; Busnel, J. M.; Wolff, P.; Francois, Y. N.; Leize-Wagner, E. *Anal. Bioanal. Chem.* **2014**, *406*, 1029–1038.
- (33) Dubois, M.; Fenaille, F.; Clement, G.; Lechmann, M.; Tabet, J.-C.; Ezan, E.; Becher, F. *Anal. Chem.* **2008**, *80*, 1737–1745.
- (34) Shen, Y. F.; Smith, R. D. *J. Microcolumn Sep.* **2000**, *12*, 135–141.
- (35) Legaz, M. E.; Pedrosa, M. M. *J. Chromatogr. A* **1996**, *719*, 159–170.
- (36) Verzola, B.; Gelfi, C.; Righetti, P. G. *J. Chromatogr. A* **2000**, *868*, 85–99.
- (37) Punzet, M.; Ferreira, F.; Briza, P.; van Ree, R.; Malissa, H., Jr.; Stutz, H. *J. Chromatogr. B* **2006**, *839*, 19–29.
- (38) Smith, R. D.; Olivares, J. A.; Nguyen, N. T.; Udseth, H. R. *Anal. Chem.* **1988**, *60*, 436–441.
- (39) Qian, J.; Liu, T.; Yang, L.; Daus, A.; Crowley, R.; Zhou, Q. W. *Anal. Biochem.* **2007**, *364*, 8–18.
- (40) Janin-Bussat, M.-C.; Tonini, L.; Huillet, C.; Colas, O.; Klinguer-Hamour, C.; Corvaia, N.; Beck, A. In *Glycosylation Engineering of Biopharmaceuticals*; Beck, A., Ed.; Humana Press: New York, 2013; pp 93–113.
- (41) Liu, H. C.; Gaza-Bulseco, G.; Faldu, D.; Chumsae, C.; Sun, J. *J. Pharm. Sci.* **2008**, *97*, 2426–2447.
- (42) Raju, T. S.; Scallon, B. J. *Biochem. Biophys. Res. Commun.* **2006**, *341*, 797–803.
- (43) Beck, A.; Wagner-Rousset, E.; Bussat, M. C.; Lokteff, M.; Klinguer-Hamour, C.; Haeuw, J. F.; Goetsch, L.; Wurch, T.; Van Dorsselaer, A.; Corvaia, N. *Curr. Pharm. Biotechnol.* **2008**, *9*, 482–501.